Polarization and Angular Distribution of the Neutrons from ^{14}C(p, n) Reaction and the Tensor Force*

C. Wong and J. D. Anderson

Lawrence Radiation Laboratory, Livermore, California 94550

and

V. A. Madsen, F. A. Schmittroth,† and M. J. Stomp

Oregon State University, Corvallis, Oregon 97331

(Received 12 October 1970)

The polarization of the neutrons from the ^{14}C(p,n) reaction leading to the first three levels of ^{14}N has been measured at six bombarding energies between 7.2 and 13.3 MeV. The polarization and angular distribution of the neutrons leading to the two 1^+ states have been analyzed with a microscopic distorted-wave Born-approximation formalism that has been extended to include spin-orbit optical distortions and a tensor component in the effective two-body force; the analog-state transition has been analyzed with the Lane model. The angular distribution and polarization shapes for the analog transition are not well reproduced by the Lane model, primarily because of lack of precise optical parameters as a function of bombarding energy. However, the integrated cross sections between 8.8 and 18.3 MeV are reasonably well accounted for with a constant real and imaginary isospin strength of 88 and 40 MeV, respectively. The corresponding real microscopic charge-exchange strength is $V_T = 9$ MeV for a Yukawa form factor of range 1.4 fm. The calculated 1^+ angular-distribution shapes are in fair agreement with measurements and are consistent with a constant central spin-spin and tensor strength between 10.4- and 18.3-MeV bombarding energy: $V_{\sigma\tau} = 7 \pm 1$ MeV and $V_T = 4.7 \pm 0.7$ MeV, although there is some indication that the tensor strength is decreasing with increasing energy. Contrary to the angular-distribution measurements, the 1^+ polarization measurements do not clearly favor a tensor component in the effective two-body force; neither the pure central nor the central-plus-tensor polarization calculation fits the data particularly well. This disagreement is probably due to optical-parameter uncertainties and contributions from second-order processes, and possibly to the neglect of tensor exchange and small admixtures of intermediate-structure resonance processes.

INTRODUCTION

In recent papers[1,2] the distorted-wave Born approximation (DWBA) with a microscopic model has been used for analysis of the (p,n) reaction data from this laboratory. It has been shown[2] that for analog transitions with even targets the microscopic model gives nearly the same result as the Lane model,[3] and the charge-exchange force $V_\tau \vec{t} \cdot \vec{\tau}$ shows consistency from one nucleus to another. For analog transitions in odd nuclei and for nonanalog transitions, the charge-exchange spin-flip interaction will play a role. The presence of spin-dependent forces was first noted[4] in the experimental observation of the ^{18}O$(p,n)^{18}$F(g.s.) $(0^+ \rightarrow 1^+)$ transition, which can proceed only by spin flip. Application of the microscopic model with purely central forces to many analog (p,n) transitions and a number of nonanalog transitions (mostly in light nuclei and which are expected to proceed primarily through $L = 0$ orbital angular momentum transfer) has yielded values of $V_\tau \approx 24$ MeV and $V_{\sigma\tau} \approx 16$ MeV for a Yukawa two-body interaction of range 1.0 fm.[2,5] For $L = 2$ transitions the required strengths are somewhat larger, $V_\tau \approx 44$ MeV. It has been shown[5,6] that the inclusion of knockout exchange reduces this discrepancy considerably: The V_τ for $L = 0$ is reduced slightly to 18 MeV, while the V_τ for $L = 2$ is reduced to ~23 MeV. The magnitudes and phases of direct and exchange amplitudes, particularly in the p shell, are fairly close to being the same, so a purely direct calculation with an L-dependent interaction strength appears adequate to "mock up" the exchange effects.

A particularly interesting application of the charge-exchange formalism is to the mass-14 system. The ^{14}C Gamow-Teller β decay, although superallowed by selection rules, is retarded experimentally by a factor of about 5000 when compared with calculations employing simple wave functions such as $(p_{1/2})^2$. It was shown by Visscher and Ferrell[7] that this inhibition could be explained by the presence of a tensor two-nucleon interaction within the context of a purely p-shell nuclear structure model. No central force mixture is capable of giving the required cancellation in the β-decay matrix element.[7,8] Rose, Häusser, and Warburton[9] have recently made a study of the effect of $2s$, $1d$

configuration admixtures and have concluded that a tensor interaction is still required to give the abnormally small β-decay rate.

The $L = 0$ contribution to the charge-exchange amplitude is very nearly proportional to the allowed β-decay matrix element.[1] Thus one would expect the $^{14}C(p,n)$ ground-state reaction to proceed primarily through transfer of $L = 2$, which is normally weaker than the $L = 0$ contribution but by no means negligible, as it is in β decay. It has been found, however, that the $L = 2$ contribution to the (p,n) reaction to the ground state of ^{14}N is too weak and in addition has an angular distribution which does not agree with the data.[1] Similar difficulties have been noted[10] in the analogous transitions $^{14}C(^3He, t)^{14}N(g.s.)$, $^{14}N(p,p')$ 2.31 MeV, $^{14}N(^3He, ^3He')$ 2.31 MeV, and $^{14}N(^3He, t)^{14}O(g.s.)$. It was concluded[1] that additional spin-dependent mechanisms such as a tensor force and/or exchange were needed to fit the $^{14}C(p,n)$ ground-state transition. The fact that the angular distribution is not changed substantially by inclusion of exchange[6,11] leads one to conclude that the tensor force is crucial in explaining the $^{14}C(p,n)$ ground-state transition. Preliminary tensor calculations,[12] with tensor-to-central strength ratios not too different from the one-pion exchange potential, seem promising: The calculated ground state and upper 1^+ integrated cross sections agree fairly well with measurements. However, the ground-state angular distribution, although considerably improved, still does not fit particularly well.

Because polarization is expected to be sensitive to the character of spin-dependent forces, we have undertaken an experimental study of the polarization of the neutron groups to the first three states of ^{14}N in the $^{14}C(p,n)$ reaction. Microscopic DWBA calculations, including spin-orbit optical distortions and central and tensor charge-exchange forces, are presented and compared with the experimental differential cross sections[1] and polarizations for the ground and 3.95-MeV 1^+ excited state transitions. In addition, the analog-state polarizations and angular distributions[1] are compared with the predictions of the Lane Model.[3]

EXPERIMENTAL METHOD

The experimental method for measuring neutron polarization has been described in detail in a previous publication.[13] Briefly, the method consists of precessing the neutron magnetic moment plus and minus 90° with a suitably designed solenoid to obtain the equivalent "left" and "right" scattering measurements. The 90° precession results from the fact that the reaction and scattering planes are at right angles to each other (see Fig. 1 of Ref.

13). The analyzer was liquid helium, and the angle of scattering from the helium was 60°. The reaction angle was varied remotely from 0 to 90° by mounting the solenoid and associated shielding on a rotating platform fabricated from a 70-mm gun mount. Figure 2 of Ref. 13 shows the solenoid and associated shielding to reduce the neutron and γ-ray background. The neutron detector was a 5×5-cm stilbene scintillator located 30 cm from the helium scatterer. Time-of-flight and proton-electron pulse shape discrimination were employed to reduce the γ background. To further reduce the background and in addition enhance the separation between electrons and protons, recoil protons were accepted only if they fell within prescribed pulse-height limits. This pulse-height "window," which is a function of bombarding energy, Q of the reaction and energy degradation of the neutrons upon being scattered from helium, was optimized for each bombarding energy and was the same for all neutron groups and all reaction angles.

A. Targets

For the lower-energy measurements, $E_p = 7.2$, 8.8, and 10.4 MeV, the gas target is as described in Ref. 13, i.e., 2.5×2.5-cm gas cell lined with Ta. The entrance window was 0.0013-cm Ta and was supported by a gold grid whose transmission was approximately 90%. The cell was filled with $^{14}CO_2$ gas to a pressure of 1.5 atm; the isotopic purity of the ^{14}C was 91%.

Above 10.4 MeV, the background neutrons from the Ta entrance window and stopper were appreciable. To extend the measurements beyond 10.4 MeV, a new 2.5×2.5-cm target with nickel entrance and exit windows was fabricated. The beam stopper was also nickel and was located some 30 cm from the gas cell. With this design and shielding arrangement (see Fig. 1) neutrons from the stopper were effectively shielded from the detector since these neutrons no longer can travel down the center of the solenoid. In addition, because of the higher Q values for the $^{58,60}Ni(p,n_0)$ reactions, neutrons from the bombardment of the nickel windows do not interfere with the $^{14}C(p,n)$ neutrons. [The ^{58}Ni and $^{60}Ni(p,n_0)$ Q values are -9.4 and -7.1 MeV, respectively, while the $^{14}C(p,n_2)$ Q value to the 3.95-MeV level in ^{14}N is -4.6 MeV.] With this new target (two atm pressure and 9-mg/cm^2 unsupported Ni windows) measurements were made at $E_p = 10.4$, 11.7, 12.6, and 13.3 MeV.

B. Measurements

At each reaction angle, four measurements were made to obtain the polarization. The order was: background and helium scattering measurements
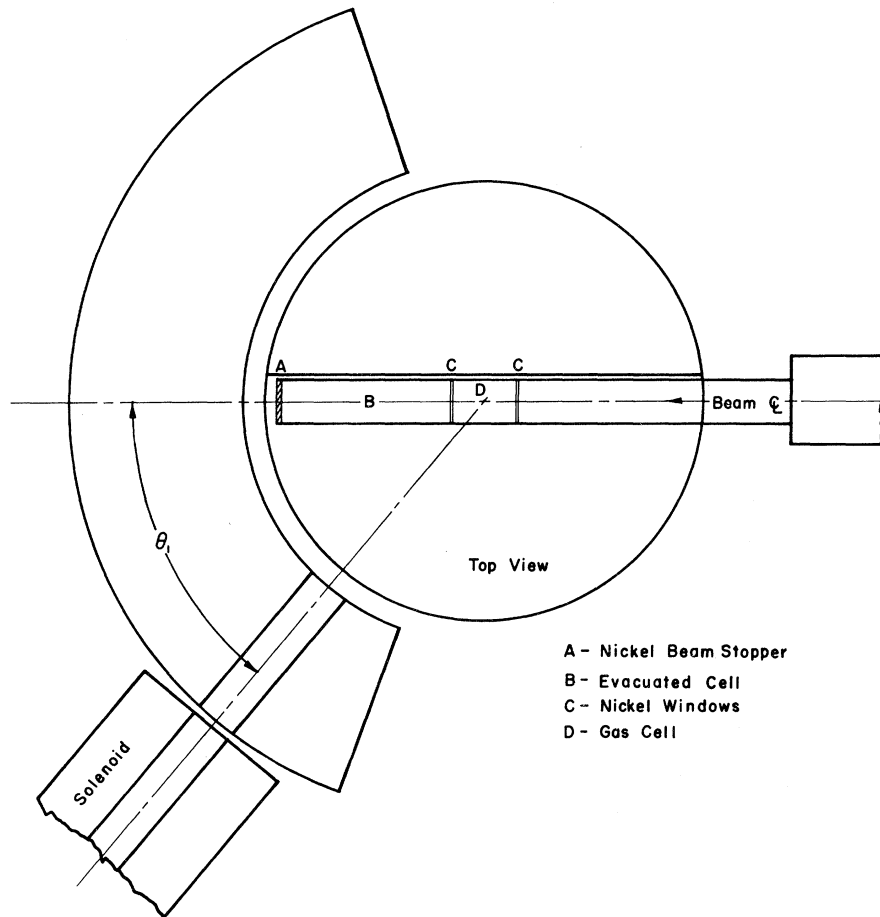
FIG. 1. Schematic draw-
ing of the target assembly
used at the higher bombard-
ing energies to reduce back-
ground.

A- Nickel Beam Stopper
B- Evacuated Cell
C- Nickel Windows
D- Gas Cell

for positive 90° precession, and then helium and
background measurements for negative 90° preces-
sion. The two helium scattering measurements
are adjacent to each other in order to minimize the
effects of any possible time drift in the electronics
and associated equipment. The background mea-
surements were obtained with an empty helium cry-
ostat. The reaction angle was varied as follows:
0°, even angles increasing to 80°, 90°, odd angles
decreasing to 10°, and another 0°. The zero de-
gree measurements always gave a null result with-
in statistics showing the absence of instrumental
asymmetries. The data from the odd and even an-
gles were consistent with each other showing ade-
quate stability of the electronics and reproducibil-
ity of the data.

The solenoid current was adjusted for 90° pre-
cession for the analog-state neutron group. Hence
the ground-state neutrons are precessed less than
90° while the neutrons leading to the upper 1^+ state
in ^{14}N at 3.95 MeV are precessed more than 90°.
Since the asymmetry parameter R is a slowly vary-
ing function of solenoid current (i.e., $R \sim \sin\frac{1}{2}\pi I/I_0$,
where I_0 is the current for 90° precession and

$I \cong I_0$), the correction in the asymmetry parame-
ter for the ground-state group and upper 1^+ group
was in general less than 3% and hence was neglect-
ed.

Figure 2 shows typical results for $E_p = 10.4$ MeV
and $\theta_1 = 20°$. The dots represent the time-of-flight
spectrum of the neutrons scattered from He while
the crosses represent the corresponding back-
ground from an empty cryostat. Figure 2(a) cor-
responds to a "left" scattering measurement (+90°
precession) while 2(b) corresponds to a "right"
scattering (−90° precession).[14] The three peaks
correspond to neutron groups leading to the ground
and first two levels of ^{14}N. Occasionally, the time-
independent backgrounds for the signal and empty
cryostat runs were different due to differing bom-
bardment times. In these cases, a correction was
applied to the net helium signal to compensate for
the differing time-independent background levels.
The asymmetry R for 90° precession is defined as:

$$R(I = I_0) = \frac{N(+\frac{1}{2}\pi) - N(-\frac{1}{2}\pi)}{N(+\frac{1}{2}\pi) + N(-\frac{1}{2}\pi)} = P_{He}P \ ,$$

where $N(\pm\frac{1}{2}\pi)$ are the net helium scattered counts

FIG. 2. Typical time-of-flight polarization data obtained from the $^{14}C(p, n)$ reaction at $\theta_1 = 20°$ and $E_p = 10.4$ MeV. The crosses represent background taken with an empty helium cryostat. The three neutrons groups n_0, n_1, and n_2 are clearly visible. (a) corresponds to a "left" scattering measurement while (b) corresponds to a "right" scattering measurement.
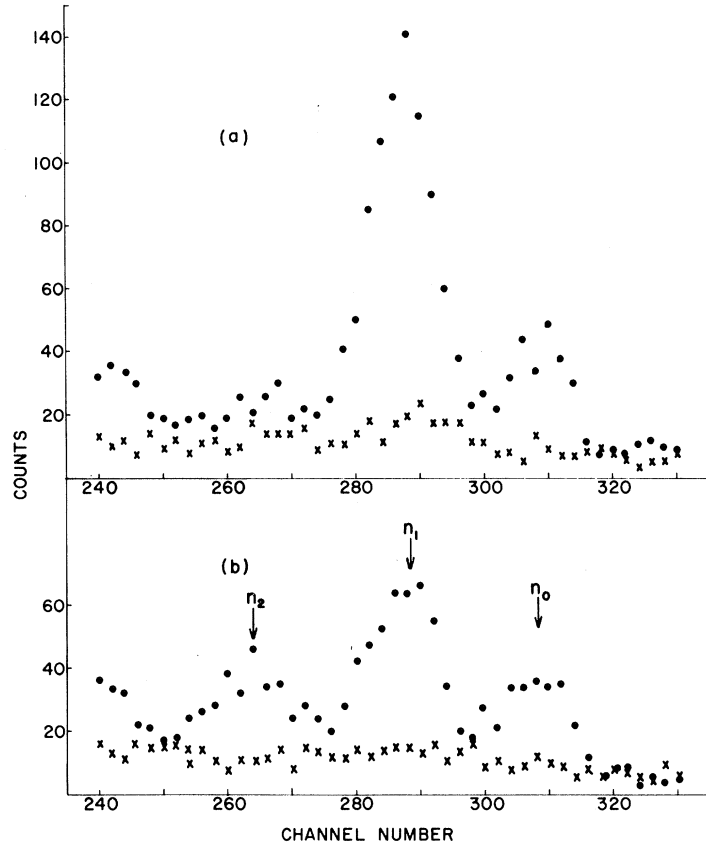
for $\pm\frac{1}{2}\pi$ precession, respectively.[15] P_{He} is the polarization of the neutrons scattered from the helium and P is the polarization of the neutrons from the (p, n) reaction.

EXPERIMENTAL RESULTS

The neutron polarizations were computed using the above equation and are shown in Fig. 3. The values of P have been corrected for multiple scattering; these corrections varied between 8 and 12%. For a discussion of the P_{He} values used and the multiple scattering calculations see Ref. 13. The error on P was computed from the statistical counting error on the product $P_{He}P$, since the statistical counting errors are much larger than the uncertainties in the values of P_{He}. The proton beam energy spread due to energy loss in the gas targets varied between ± 0.18 MeV at $E_p = 7.2$ MeV and ± 0.14 MeV at $E_p = 13.3$ MeV.

Figure 3 shows that the ground-state neutron polarizations vary slowly with energy; with the exception of the 13.3-MeV data, the polarizations are negative at the forward angles ($\theta \lesssim 60°$). The upper 1^+ state neutron polarizations exhibit a similar behavior if one were to exclude the data at 10.4 MeV.

The 10.4-MeV data exhibit an anomalous behavior in that the polarizations are positive out to $\theta = 60°$. The analog-state neutron polarizations show little energy dependence up to 10.4 MeV; the polarizations are negative at the forward angles and positive beyond 60°. Between 10.4 and 13.3 MeV, the energy dependence is more rapid. At 12.6 MeV, the analog-state neutron polarizations exhibit an additional positive peak in the region of $\theta = 40°$, which can be seen slowly evolving in the 11.7-MeV data. At 13.3, the positive peak at $\theta = 40°$ is still evident but smaller. However, the polarization at $\theta = 10°$ is now positive, which is quite unexpected.

THEORY

In this section we present a formulation[16] of the nonexchange scattering of a composite projectile of internal wave function $\phi_{J'T'}^{M_i'P_i'}$ by a nucleus with internal wave function $\phi_{J_iT_i}^{M_iP_i}$ through both central and tensor two-nucleon forces. The internal wave function of the projectile is assumed to be purely S-state and we consider only elastic or quasielastic processes for the projectile. The internal spatial wave function of the projectile is factored from the spin-isospin part of the wave function and folded into the two-nucleon interaction, re-

sulting in an interaction of the same character but with a different radial shape. This has been carried out[17] for a central force but may also be done for a tensor force with similar results. We assume that the spatial part of the interaction is the result of such a procedure. The resulting effective interaction is with the center of mass of the projectile; however, the spin-isospin operators act on individual nucleons in the projectile and those in the target.

The notation is nearly the same as in Ref. 17. Projectile coordinates and quantum numbers are

denoted by primes. Conserved quantum numbers are denoted by i and f and those which are to be summed over by 1 and 2 in the initial and final states, respectively. The circumflex is used for unit vectors ($\hat{r} = \vec{r}/r$), and for the abbreviation $\hat{J} = (2J+1)^{1/2}$.

The detailed calculation of the scattering amplitude including a tensor interaction is presented in the Appendix. The result is

$$A_{M_i M'_i, M_f M'_f} = \sum_{IN} C(J_i J_f I; M_i - M_f - N)(-1)^{J_i - M_i}$$
$$\times \alpha(M'_i M'_f IN), \tag{1}$$

where

$$\alpha(M'_i M'_f IN) = \sum_{L_1 L_2 M J_1 J_2 I' L} (4\pi)^2 i^{L_1 - L_2}(-1)^{N + I - I' - L} Y^0_{L_1}(\hat{0}) Y^M_{L_2}(\hat{k}_f) C(L_1 J' J_1; 0 M'_i M'_i)$$

$$\times C(L_2 J' J_2; M, M'_f, M + M'_f)(-1)^{J_1 - M'_i} C(J_1 J_2 I; M', -M - M'_f, N) \frac{\hat{J}_1 \hat{J}_2 \hat{I}'}{\hat{I}} \begin{pmatrix} J_1 & J' & L_1 \\ J_2 & J' & L_2 \\ I & I' & L \end{pmatrix} \langle L_2 \| Y_L \| L_2 \rangle$$

$$\times \int \mathcal{R}_{J_2 L_2}(R') G_{II'L}(R') \mathcal{R}_{J_1 L_1}(R') R'^2 dR', \tag{2}$$

where the $\mathcal{R}_{JL}$ are distorted radial wave functions and $G_{II'L}(R')$ is the radial form factor Eq. (A28). From Eq. (1) we obtain a differential cross section which is coherent in I' and L but incoherent in IN:

$$\frac{d\sigma}{d\Omega} = \left(\frac{2m}{4\pi\hbar^2}\right)^2 \frac{k_f}{k_i} \frac{1}{(2J+1)(2J'+1)} \sum_{INM'_iM'_f} |\alpha(M'_i M'_i IN)|^2. \tag{3}$$

In a problem where the spin-dependent distorting potentials can be neglected the dependence of the radial wave functions on J_1 and J_2 will disappear. The resulting cross section is incoherent in I, I', and L:

$$\frac{d\sigma}{d\Omega} = \left(\frac{2m}{2\pi\hbar^2}\right)^2 \frac{k_f}{k_i} \frac{1}{(2J_i+1)(2J'+1)}$$
$$\times \sum_{II'LM} |\langle \chi_f^{(-)} | G_{II'L}(R') Y^M_L(R') | \chi_i^{(+)} \rangle|^2, \tag{4}$$

where the χ are purely spatial distorted wave functions.

The polarization can be calculated[18] from the amplitude Eq. (1). Assuming that the initial beam and target are unpolarized, the polarization is

$$\frac{\langle J'_Y \rangle}{J'} = \frac{\displaystyle\sum_{IM_iN} \text{Im}[\alpha(M'_i M'_f IN)\alpha^*(M'_i M'_f + 1, IN)]}{J' \displaystyle\sum_{INM'_iM'_f} |\alpha(M'M'IN)|^2} . \tag{5}$$

This is the only nonzero component of the polarization if the y axis is chosen along $\hat{k}_i \times \hat{k}_f$.

It is worthwhile to point out some features of the scattering amplitude with the inclusion of a tensor

interaction. First, it is seen that the tensor force is purely spin flip, $I' = 1$. For the spin-flip amplitudes and for a given total angular momentum transfer I and isospin transfer τ the contribution from a given λ of the central and tensor terms are proportional except for differences in the radial function; that is, all the $j_1 j_2$ dependent factors are the same. The effect of the particular configuration mixture on a transition rate will be expected to be nearly the same for both central and tensor terms of a given value of the nuclear orbital transfer λ. However, the projectile orbital transfer L need not be equal to λ as for a purely central force but may be seen to have other possibilities. The restrictions satisfied by the various transfer quantum numbers are:

$$|J_i - J_f| \leq I \leq |J_i + J_f|$$

$$|T_i - T_f| \leq \tau \leq |T_i + T_f|$$

$$|j_1 - j_2| \leq I \leq |j_1 + j_2|$$

$$|l_1 - l_2| \leq \lambda \leq |l_1 + l_2|$$

$$|I - I'| \leq L \leq |I + I'|$$

$$|I - I'| \leq \lambda \leq |I + I'|$$

$$L = \lambda \quad \text{(central force)}$$

$$L = \lambda, \lambda \pm 2 \quad \text{(tensor force)}$$

$$0 \leq I' \leq 1$$

$$0 \leq \tau \leq 1$$

$$(-1)^\lambda = (-1)^L = (-1)^{\Delta\pi}. \tag{6}$$

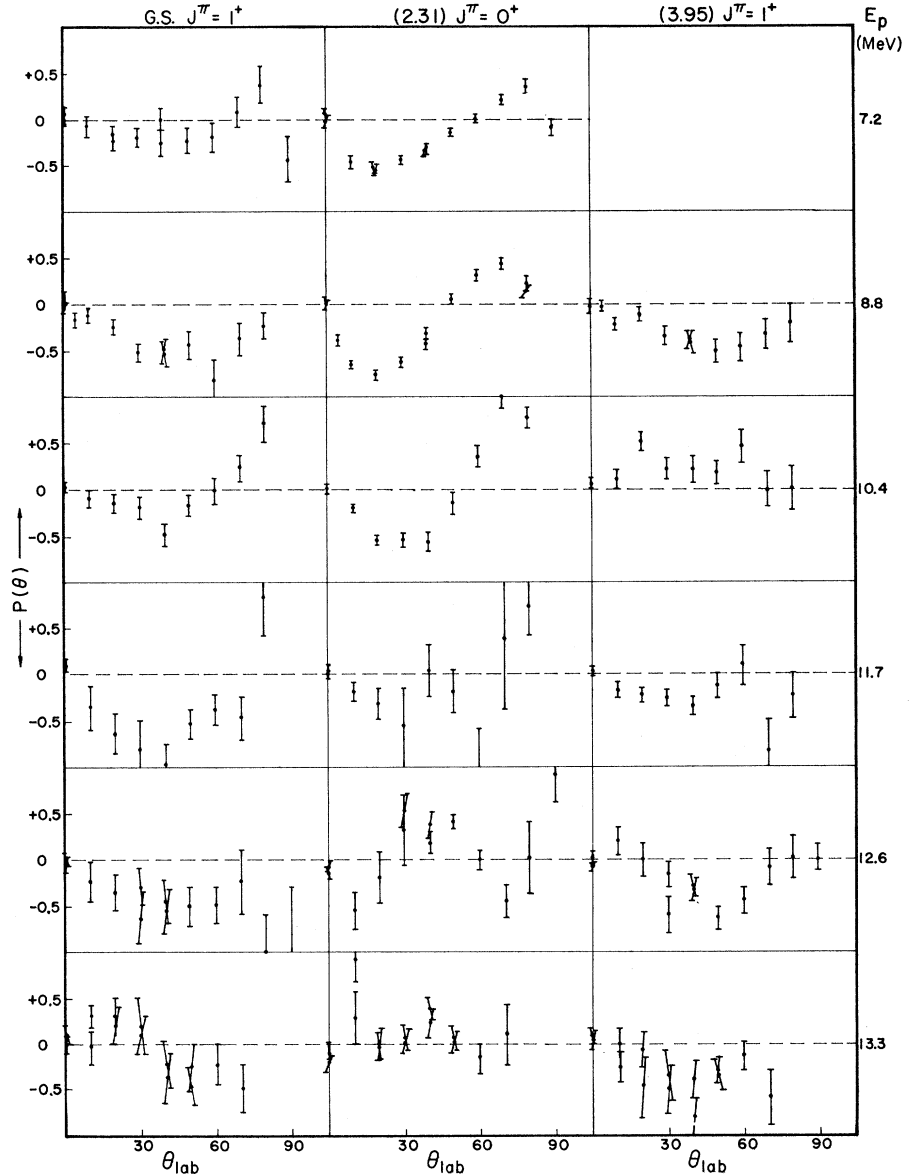It is possible to show that for the tensor force

FIG. 3. Polarization for the three neutron groups as a function of bombarding energy.

radial form factor [Eq. (A6)], the central and tensor terms in the amplitude for which $\lambda = L$ are constructively coherent, assuming that the signs of central and tensor strengths are the same. The sign of the $\lambda \neq L$ terms relative to the $\lambda = L$ terms is is not definite but depends on the single-particle transition. It is destructive for $j_1 = l_1 \pm \frac{1}{2} \to j_2 = l_2 \pm \frac{1}{2}$ and constructive for $j_1 = l_1 \pm \frac{1}{2} \to j_2 = l_2 \mp \frac{1}{2}$. One must also include the short-range subtractive term in the tensor force, Eq. (7). However, because of the absorptive optical potential the long-range term will tend to dominate, particularly in the (^{3}He, t) reaction.

As an example of the extra freedom permitted by the tensor force, consider a transition with a

model wave function consisting purely of $P_{3/2}$-shell configurations. For a $0^+ \to 3^+$ transition the relation $L = I - I'$ and the parity rule would permit $L = 2, 4$. For a central force only $L = \lambda = 2$ is possible, but for a tensor force L may be both 2 and 4. Another example in which the tensor force plays an important role, is the case of ^{14}C(p, n)-^{14}N(1^+ g.s.). The transition is purely $I' = \tau = 1$, and I is restricted to a single value 1. The possible orbital transfers are $\lambda = 0, 2$; $L = 0, 2$. With only a central force, the $L = \lambda = 0$ term in the amplitude is nearly proportional to the β-decay matrix element, and is therefore very small. This transition is then dominated by the $L = \lambda = 2$ term. When a tensor force is also included we have the possibil-

ity of having both $L = 0$, $\lambda = 2$ and $L = 2$, $\lambda = 2$, the $L = 2$, $\lambda = 0$ being very small. The $L = 0$, $\lambda = 2$ dominates for the forces used in calculations presented in the analysis section.

ANALYSIS

A. Method of Calculation

The analysis for the analog state has been done using the Lane Model[3] with optical parameters taken from the work of Watson, Singh, and Segel.[19] Calculations were carried out with the LOKI[20] coupled-channel code using a macroscopic form factor which includes a complex isospin term.[19] The results are very nearly the same as would be ob-

tained with DWBA, the multiorder feature of coupled-channel calculations not being important for the analog transition.

For the transitions to the two 1^+ states a microscopic coupled-channel code has been used. However, it has been made equivalent to DWBA by scaling down the interaction strengths. Channel-coupling effects will be considered separately in a later publication.

In all cases the tensor force used in the calculations had the one-pion range, $\alpha = 0.714$ fm^{-1}, and a "regularizing" term with inverse range $\beta = 4$ fm^{-1} which was subtracted to remove the r^{-3} singularity in the radial form factor. The resulting form factor,

$$V_{L\lambda} \propto \begin{cases} j_\lambda(i\alpha r_1)h_L^{(1)}(i\alpha R') - (\beta^3/\alpha^3)j_\lambda(i\beta r_1)h_L^{(1)}(i\beta R') & R' > r_1 \\ j_L(i\alpha R')h_\lambda^{(1)}(i\alpha r_1) - (\beta^3/\alpha^3)j_L(i\alpha R')h_\lambda^{(1)}(i\alpha r_1) & R' < r_1, \end{cases} \qquad (7)$$

is continuous with a finite discontinuity in the first derivative at $R' = r_1$ whereas either term by itself is discontinuous at $R = r'$. The expansion Eq. (A6) of the one-pion potential is not correct, because of the r^{-3} singularity, unless this subtractive term

is included.

B. Analog Transition

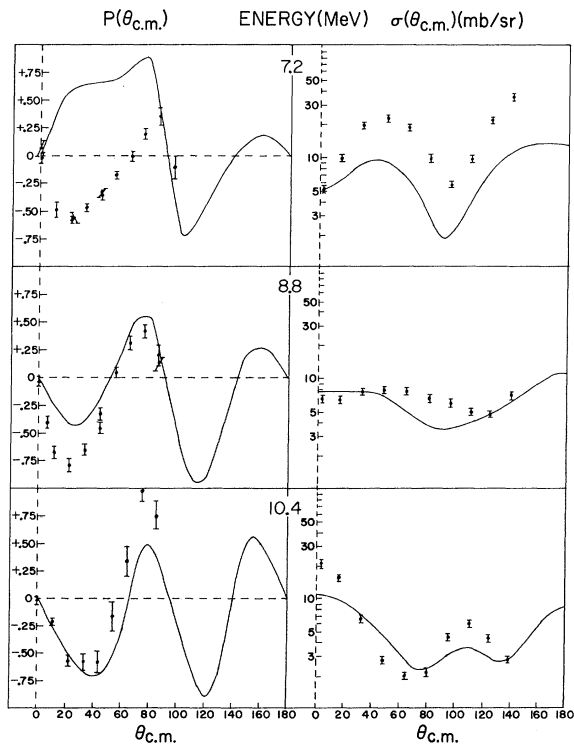Since optical parameters as a function of bombarding energy are not available for protons on

FIG. 4. Polarization and angular distribution of neutrons leading to the analog state (n_1). The solid lines are the Lane Model predictions.
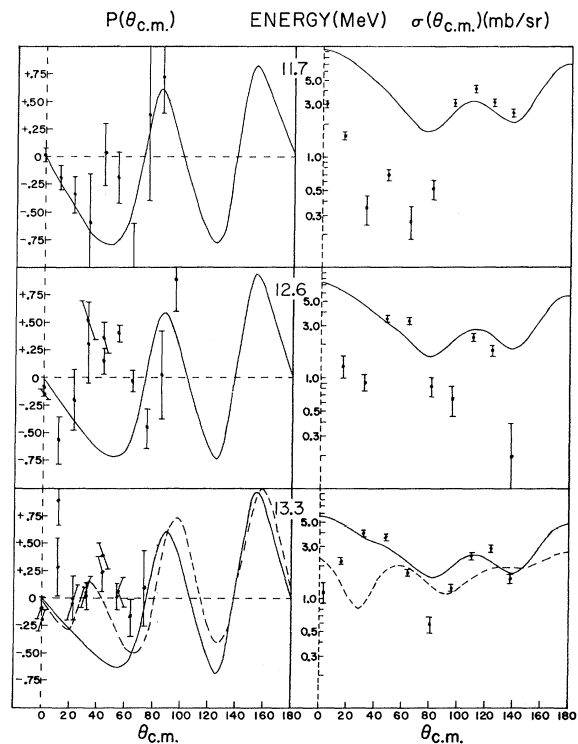

FIG. 5. Polarization and angular distribution of neutrons leading to the analog state (n_1). The solid lines are the Lane Model predictions.

[14]C, the generalized neutron and proton optical parameters deduced by Watson, Singh, and Segel[19] for p-shell nuclei were used. The Watson parameters (in an obvious notation) are:

Protons:

$$V_R = 60.0 + 0.4\frac{Z}{A^{1/3}} + 27\frac{N-Z}{A} - 0.3E_{c.m.},$$

$$V_{so} = 5.5,$$

$$r_{so} = r_R = r_I = 1.15 - 0.001E_{c.m.},$$

$$\alpha_R = \alpha_{so} = 0.57, \quad \alpha_I = 0.5,$$

$$W_S = W_S(E) + 10.0(N - Z/A),$$

$$W_V = W_V(E),$$

Neutrons:

$$V = 60.0 - 27(N - Z/A) - 0.3E_{c.m.},$$

$$W_S = W_S(E) - 10(N - Z/A),$$

where

$$W_V = 0 \text{ for } E_{c.m.} < 32.7 \text{ MeV}$$

and

$$W_S = 0.64E_{c.m.}, \qquad E_{c.m.} < 13.8 \text{ MeV},$$
$$= 9.60 - 0.06E_{c.m.}, \qquad E_{c.m.} \geq 13.8 \text{ MeV}.$$

The above symmetry dependence for both the real and imaginary potentials implies a complex $(\vec{t}\cdot\vec{\tau})$ interaction in the Lane Model. The equivalent real $(\vec{t}\cdot\vec{\tau})$ strength is 108 MeV while the imaginary $(\vec{t}\cdot\vec{\tau})$ strength is 40 MeV. In the calculations, the imaginary $(\vec{t}\cdot\vec{\tau})$ strength was set equal to 40 MeV and the form factor was identical to that for the imaginary potential, i.e., derivative Woods-Saxon. The real $(\vec{t}\cdot\vec{\tau})$ strength and form factor were deduced from a microscopic DWBA calculation with $V_\tau = 9$ MeV of the [14]C(p,n) analog transition.[1,2] The deduced strength was 88 MeV; the Woods-Saxon form factor was slightly different from that for the real potential (the radius parameter was 1.16 fm compared to 1.14 fm while the diffuseness was 0.95 fm compared to 0.57 fm). The real and imaginary neutron and proton optical parameters inserted into the code neglected the symmetry dependence since the diagonal matrix elements of $(t\cdot\tau)$ are computed in LOKI. For the spin-orbit term the form factor was of the Thomas-type, i.e. $(1/r)dV_R/dr$, whereas Watson et al. employed $(1/R_{so})dV_R/dr$. The Watson form preserves the surface-type feature of the spin-orbit force for very light nuclei $(A \cong 6)$. For $A = 14$, the difference between the form factors is less and hence it is expected that the effect on the calculation is minimal.

The differential cross sections and polarizations for the analog-state transition were calculated for nine bombarding energies between 7.2 and 18.3 MeV. The predictions are shown in Figs. 4–6 as solid lines together with the measured polarizations and differential cross sections.[1]

C. 1[+] Transitions

Calculations of the differential cross sections have been carried out for the transitions to the 1[+] ground state and to the 3.95-MeV 1[+] state of [14]N. For these transitions no macroscopic treatment is possible, and the microscopic model including a tensor term in the two-nucleon interaction has been used. The spectroscopic amplitudes occurring in Eq. (A28) require a specific microscopic-model description for the nuclear states. As in previous studes,[1] we have used Visscher-Ferrell[7] wave functions.

The comparison of the theoretical cross sections to experiment is shown in Figs. 7 and 8 at bombarding energies of 10.4, 12.0, 13.3, and 18.3 MeV. The strengths of $V_{\sigma\tau}$ and V_T used in the calculations are shown for each energy, and by comparison calculations using a purely central force are shown at some of the energies.

As discussed in the theory section, the tensor force is expected to have a large effect on the g.s.
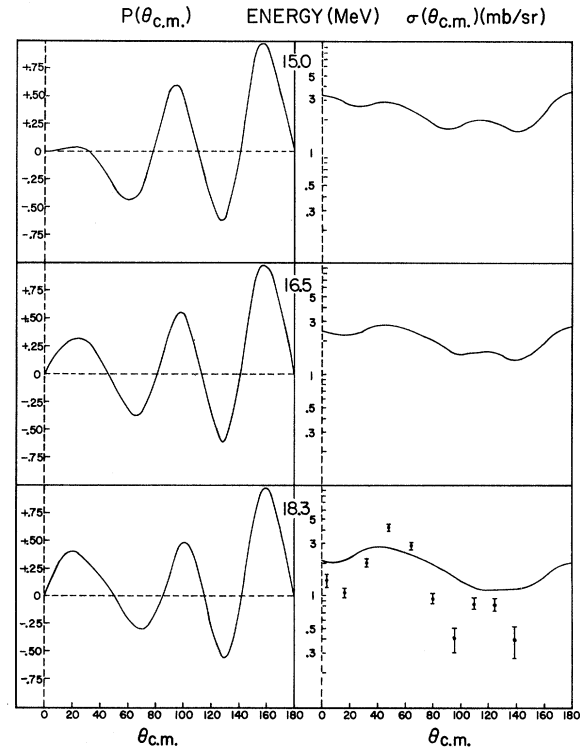

FIG. 6. Polarization and angular distribution of neutrons leading to the analog state (n_1). The solid lines are the Lane Model predictions.

cross section because of the inhibition of the $\lambda = 0$ nuclear amplitude, which is also responsible for the near vanishing of the β-decay matrix element. Thus, the normally dominant $\lambda = 0$, $L = 0$ central force contribution is expected to be nearly zero. For the transition to the 3.95-MeV state the situation is just reversed: the $\lambda = 0$ amplitude is large while the $\lambda = 2$ amplitude is small. The central $L = 0$, $\lambda = 0$ part of the amplitude should be dominant.

As expected the cross sections for the 3.95-MeV state (Fig. 7) are not much changed by the inclusion of the tensor force. Its effect for the $L = 0$ term is to decrease the cross section slightly without affecting the angular distribution but to increase greatly the $L = 2$ contribution. The change
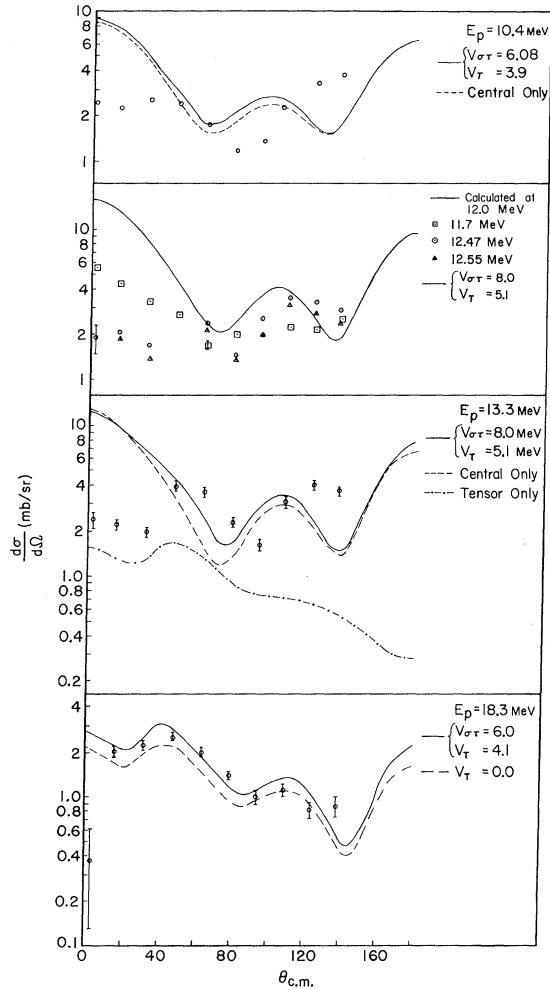
in the $L = 0$ term comes from the $\lambda = 2$ nuclear multipole, while the change in the $L = 2$ part of the cross section comes primarily from the $\lambda = 0$ multipole, which is strong.

The experimental and calculated cross sections for the 1^+ ground-state transition are shown in Fig. 8. The large effect of the tensor component in the two-body interaction improves greatly the fit to the magnitude and angular distribution for
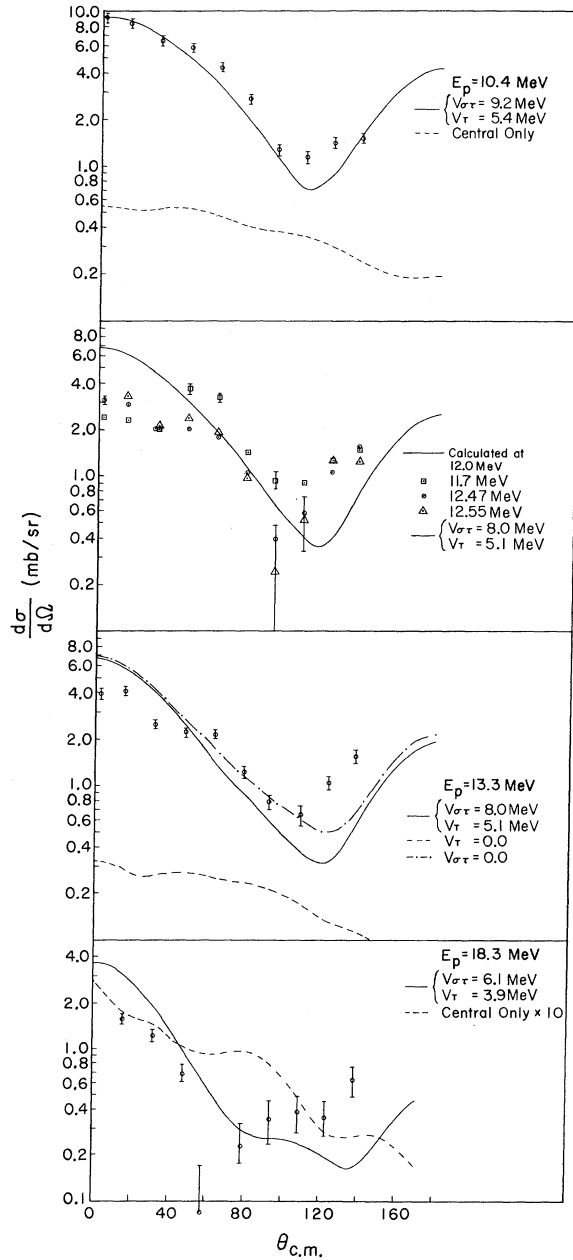

FIG. 7. Differential cross sections for ^{14}C(p,n) leading to the 3.95-MeV 1^+ state of ^{14}N(n_2). Calculations with the tensor interaction use the radial form factor with $\alpha = 0.714$ fm^{-1} and $\beta = 4$ fm^{-1}. The central form factor was a Yukawa with $\alpha = 0.714$.

FIG. 8. Differential cross sections for ^{14}C(p,n) leading to the ground state of ^{14}N(n_0).

the transition to this state.

Polarization of the neutrons was measured at six energies between 7.2 and 13.3 MeV. The data at 10.4, 12.0, and 13.3 MeV are shown along with the calculations in Figs. 9 and 10. In general, the calculated curves change little in character from energy to energy whereas the data change fairly rapidly.

DISCUSSION

A. Analog Transition

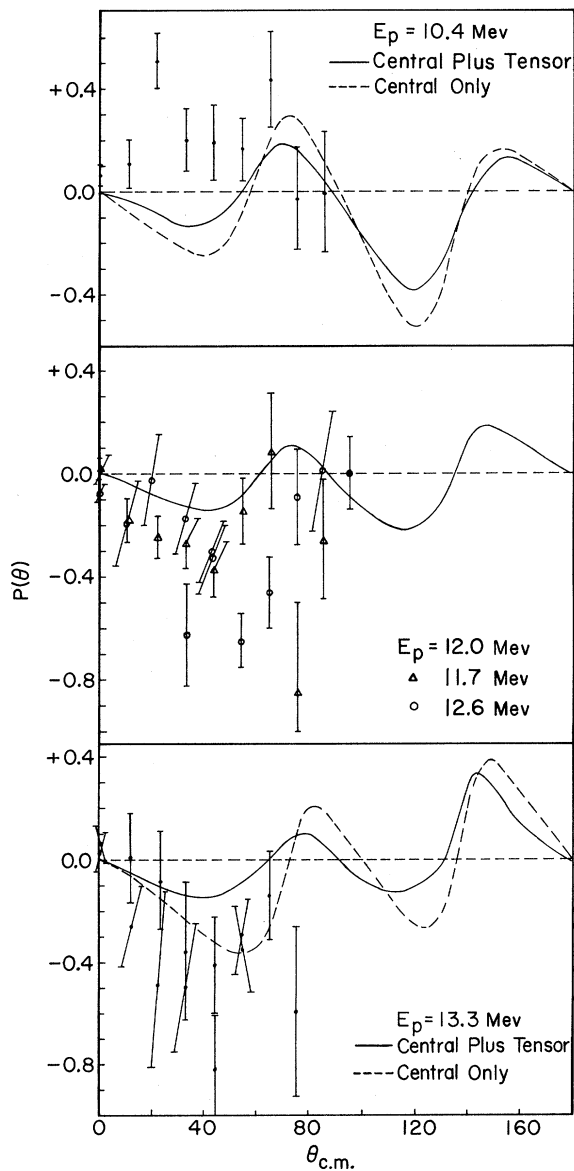From Figs. 4–6 it is seen that the agreement

between measurements and calculations is good at 8.8 and 10.4 MeV and poor at the other energies. The disagreement at 7.2 MeV is not unexpected since the Watson parameters are only valid above ≈ 10 MeV (while the neutron energy is ≈ 4 MeV) and since the integrated cross sections[1] show evidence for sizeable resonance contribution at this

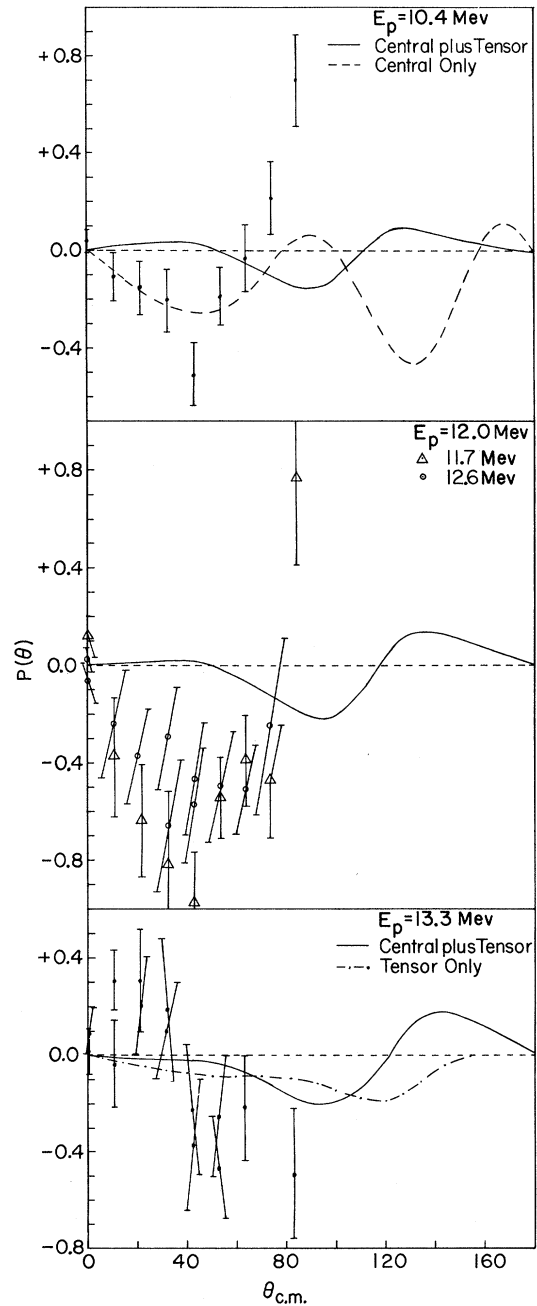FIG. 9. Polarization for the neutrons leading to the 1^+ 3.95-MeV state.

FIG. 10. Polarization for the neutrons leading to the 1^+ ground state.

energy. It is interesting to note that at 8.8 and 10.4 MeV, where the angular distributions are reasonably well described, the calculated polarizations agree fairly well with the measurements. Conversely, at 12.6 MeV at the forward angles, where the angular distributions are in poor agreement, the calculated polarizations have the wrong character. It would thus appear that if the optical parameters and isospin form factors were sufficiently accurate to predict the angular distributions then the calculated polarizations would also agree with the measurements.

Although the calculated angular distribution shapes above 10.4 MeV are in poor agreement, the integrated cross sections are reasonably well accounted for between 8.8 and 18.3 MeV using constant real and imaginary isospin strengths of 88 and 40 MeV, respectively. Since the isospin strength is expected to be constant and since the square of the strength deduced from the analysis is approximately proportional to the product of the depths of the imaginary proton and neutron optical potentials, this would imply that the energy dependence of the imaginary potentials deduced by Watson *et al.* is reasonably correct.

The poor shape agreement above 10.4 MeV is due to lack of knowledge of the optical parameters as a function of bombarding energy and/or contributions from nondirect processes. The preliminary evidence would seem to indicate the poor agreement is due primarily to lack of knowledge of the optical parameters and isospin form factors because, first and foremost, the agreement is poorer at the higher bombarding energies where nondirect processes presumably should be less important. Secondly, the energy dependence of the polarizations and angular distributions is sufficiently slowly varying to be describable with an optical model with smoothly varying energy-dependent parameters: Measurements and calculations, likewise, can change significantly for bombarding energy changes of 1–2 MeV as evidenced by the calculations at 13.3 and 15 MeV and the measurements at 10.4 and 11.7 MeV. Thirdly, the predictions are quite sensitive to optical parameters and isospin form factors. For example the dashed curves at 13.3 MeV were calculated for a surface real isospin form factor and optical parameters deduced from neutrons on nitrogen.[21] Fourthly, the magnitude of the integrated cross sections between 8.8 and 18.3 MeV can be accounted for with a direct reaction model, i.e., Lane model with a constant isospin strength. Indeed, the calculated cross section is a factor of 2 lower than the measurements at 7.2 MeV, which is suggestive that compound processes are important only at this energy. In addition intermediate-structure reso-

nance contributions,[22] if present above 8.8 MeV, cannot be large since the isospin strength is roughly constant as a function of bombarding energy. Lastly, the agreement at 10.4 MeV is probably not fortuitous and shows that the Lane model can simultaneously predict the correct (p, n) angular distributions and polarizations. In order to produce better agreement between measurements and calculations, elastic scattering data and polarization measurements are needed for ^{14}C plus proton to determine the optical parameters as a function of bombarding energy.

B. 1$^+$ Transitions

Since the optical parameters are not sufficiently accurate to predict the shape of the analog-state angular distributions and polarizations as a function of bombarding energy, a relevant question is its effect on the 1$^+$ angular distributions and polarizations. Since the DWBA and Lane Model calculations for the analog state are equivalent and since the single-particle transition amplitudes are independent of j_1 and j_2 for the p shell, it is concluded that the calculated shapes for the upper 1$^+$ angular distribution and polarizations should also be in error by the same amount. This follows directly from the fact that the upper 1$^+$ transition proceeds mainly via the central spin-spin interaction which, like the charge-exchange interaction, assumes a Yukawan form factor. The ground-state transition which proceeds via the tensor force, should also be affected but *a priori* it is not known whether it is more or less sensitive to optical parameters. However, since the square of the interaction strengths is proportional to the product of the depths of the imaginary proton and neutron potentials, it is felt that the strengths of V_T and $V_{\sigma\tau}$ are meaningfully determined, since the same imaginary strengths predict the correct analog-state cross sections.

The calculations for the 1$^+$ transitions were carried out above 10.4 MeV because nondirect processes should be less important at the higher bombarding energies. The inconsistency between the calculated cross sections to the two 1$^+$ states and experiment can be removed by the introduction of a tensor force. That the magnitude of both cross sections can be fit is not surprising since the upper-state transition proceeds almost entirely through the central force and the ground-state transition through the tensor force. The tensor strength is therefore obtained from fitting the ground-state cross section. (Thus it is not significant that the central and tensor strengths used in the calculations for the upper and lower 1$^+$ states are not always the same.) However, the central strength so determined ($V_{\sigma\tau} = 7 \pm 1$ MeV) is

consistent with the $V_{\sigma\tau}$ obtained from other transitions,[2] so it is not really a free parameter. For the ground-state transition the tensor force not only raises the magnitude but also changes the angular distribution from one of clearly the wrong character to one which is a fair fit of the data. It would thus appear that the ground-state transition is less sensitive to optical parameters and the neglect of tensor exchange. The data at 18.3 MeV are beginning to resemble the angular distribution for $^{14}N(p_{25\ \text{MeV}}, p'_{2.31\ \text{MeV}})$, which is essentially the inverse reaction. The interaction strength is $V_T = 3.9$ MeV, $V_{\sigma\tau} = 6.1$ MeV, which is close to the values $V_T = 3.9$ MeV and $V_{\sigma\tau} = 6.3$ MeV determined from the $^{14}N(p, p')$ experiment.[23] However, the latter strength was calculated with a regularizing term $\beta = 2$ instead of $\beta = 4$ (as was the present case); from calculations, the resulting strength is weaker by about a factor of 1.6. Thus the strength of the tensor force from the (p, p') experiment is about 2.44 MeV using our potential form factor with $\beta = 4$.

As expected from optical-parameter uncertainties, the transition to the 3.95-MeV state shows an angular distribution which at the lower energies is not reproduced well by the central force calculations, and the inclusion of the tensor force does not significantly change the calculated angular distributions. It is interesting to note that the pure tensor calculation does have the dip at forward angles seen in the measurements; but the magnitude of the tensor contribution is small compared to the central and makes no significant difference in the angular distribution at forward angles. Inclusion of central exchange[12] also does not reproduce this dip at the forward angles. It can be obtained using an extremely short-range force – about $\frac{1}{3}$ fm, but this would be unrealistic. The fit to the measurements at 18 MeV is good,

except that the dip at 3° is not reproduced.

In Fig. 7, the measured cross sections to the upper 1⁺ state at the forward angles show considerable fluctuation between 11.7 and 12.47 MeV. At 3° there is roughly a factor of 2 change in cross section for 800-keV change in bombarding energy. Similar fluctuations are seen in the analog-state transition but at 50° rather than 3°. Fluctuations due to compound or intermediate processes typically affect angular distributions much more strongly than total cross sections. A resonance in a particular partial wave, for example, interferes with the direct contribution of only that partial wave in the total cross section but interferes with the entire direct amplitude in the angular distribution. Thus it is reasonable that our empirical strengths V_T and $V_{\sigma\tau}$ are nearly constant in an energy range where the angular distributions fluctuate somewhat.

Table I summarizes the tensor strengths used for fitting the $^{14}C(p, n)$ reaction at various energies and the analogous $^{14}N(p, p')$ 2.31-MeV reaction.[23] Also shown are strengths found in other ways. Visscher and Ferrell[7] used the one-pion force in the shell-model study of the mass-14 system to explain the ^{14}C long-lived β decay. In order to compare this strength with others shown, the r^2 weighted volume integrals of the radial form factor have been calculated. The tensor force always selects relative orbital angular momenta differing vectorially by at least two units, so the r^2 weighting is reasonable, and it gives a finite result for the one-pion force. Also shown is a tensor force strength of the regularized type[24] with $\beta = 4$, determined by Schmittroth[12] from a central-plus-tensor parametrization of Cohen and Kurath's p-shell nuclear matrix elements[25] involving only 0^+, $T = 1$ and 1^+, $T = 0$ states. As these are the kinds of states involved in Visscher and

Table I. Tensor strengths.

Determination	Regularizing term β	Strength (MeV)	r^2 integral (MeV fm⁴)
10.4 MeV $^{14}C(p,n)$	4	5.4	1800
12.7 MeV $^{14}C(p,n)$	4	5.1	1730
13.3 MeV $^{14}C(p,n)$	4	5.1	1730
18.3 MeV $^{14}C(p,n)$	4	3.9	1305
25 MeV $^{14}N(p,p')$	2	3.9	760
Visscher-Ferrell (one pion)	none	3.7	2380
Schmittroth [a]	4	5.1	1730
Love et al. [b]	1.92	2.08	404

[a]Determined (Ref. 12) from Cohen-Kurath's p-shell matrix elements involving only $1^+ T = 0$ and $0^+ T = 1$ states.

[b]Determined (Ref. 27) by matching even parts of the Hamada-Johnston potential cutoff below the separation distance to a regularized one-pion form.

Ferrell's work, the strengths should be consistent. Comparison of the r^2 weighted integrals shows that the one-pion force is a little stronger. These two force strengths are also reasonably close to those obtained from the $^{14}C(p, n)$ reaction. This agreement is comforting, but should probably not be taken very seriously. It was also shown[12] that when all the p-shell matrix elements were used a weaker tensor strength was obtained. The same parametrization[12] in the sd shell[26] yields a tensor force of the opposite sign. Thus while the tensor force is clearly needed in nuclear-structure calculations[9] it is not consistently determined by empirical matrix elements. On the other hand, the even central strengths are consistently determined from the central-plus-tensor parametrization.[12]

Also shown is a tensor force strength recently determined from the even parts of the Hamada-Johnston potential by Love, Parish, and Richter[27] by matching low Fourier components of the G matrix to a regularized form. This force is considerably weaker than the others shown in Table I. The central charge and spin exchange strength, determined in a similar way by Love et al., is also weaker than that determined empirically from (p, n) reactions and that determined by Petrovich et al.[28] to give equivalent scattering to the Kallio-Kolltveit G matrix. In addition, Love et al. showed that the tensor force cross sections were reduced rather than enhanced by the inclusion of exchange. On the basis of their results, the strengths in Table I would have to be increased by about 40% to get agreement with the data if exchange were included.

The inclusion of the tensor force does not produce any improvement in the polarization calculations. For cases where there is a large difference between central and central-plus-tensor calculations, the latter is usually worse. This is true of the g.s. transition at 10.4 MeV and the 3.95-MeV transition at 13.3 MeV. The calculations in any case, but particularly with a tensor force, produce too little polarization compared to the measurements. Polarization is much more sensitive to optical-parameter uncertainties and small admixture of nondirect processes than the differential cross section. It is therefore not surprising that the quality of the fits to the measured polarization is poorer and that the calculated energy dependence is less rapid. In light nuclei even for elastic scattering at the higher energies, where nondirect processes are expected to be negligible, it is difficult to obtain simultaneous fits to differential cross sections and polarizations.[29] It is possible that the inclusion of tensor exchange amplitudes[27] could have a significant effect on the

polarization. No such work has been reported, but central force calculations have shown significant differences when exchange is included.[30] It is very doubtful, however, that the character of the polarization would be affected enough to produce agreement with experiment from the exchange amplitude alone. Preliminary results with coupling of the analog and the two 1^+ states in ^{14}N to the ground state of ^{14}C show that the coupling can have a significant effect on the polarization without greatly changing the differential cross section. It is clear from the calculated polarizations that they are strongly affected by the presence of a tensor two-body force, but it seems that a much more sophisticated calculation will be needed to be able to fit charge exchange polarization data.

CONCLUSIONS

Although at some of the energies the agreement of experimental and calculated angular distributions is poor, the effective-interaction parameters determined are fairly consistent. The angular distributions for the ground-state transition clearly require a tensor interaction. Between 10.4 and 18.3 MeV the V_τ and $V_{\sigma\tau}$ strengths are constant: $V_\tau = 9$ MeV while $V_{\sigma\tau} = 7 \pm 1$ MeV for a Yukawa two-body interaction of range 1.4 fm. These strengths are consistent with those determined from a model-independent analysis of the ratio of (p, n) cross sections for the lithium isotopes,[31] where it was concluded that $V_{\sigma\tau}/V_\tau = 0.66 \pm 0.08$ and is independent of bombarding energy from 10–20 MeV. The tensor strength V_T decreases monotonically from 5.4 MeV at 10.4 MeV to 3.9 MeV at 18.3 MeV. Considering the uncertainties in the determination of V_T, the present results are consistent with a constant tensor strength $(V_T = 4.7 \pm 0.7$ MeV). The poor shape agreement on some of the angular distributions may be due to lack of precise optical parameters as a function of bombarding energy and to the neglect of other possible reaction mechanism, e.g., the two-body spin-orbit force. The effects of intermediate-structure resonances on the extracted strengths of V_τ, $V_{\sigma\tau}$, and V_T cannot be large, since these strengths are roughly constant between 10.4- and 18.3-MeV bombarding energy.

In contrast to the angular distribution measurements, the polarization measurements for the 1^+ transitions do not clearly favor a tensor component in the effective two-body force. That the pure central calculation is preferred at some energies is probably not significant since the central calculation, in itself, does not fit particularly well. This lack of agreement is understandable since polarization is much more sensitive than the an-

gular distributions to optical parameter uncertainties and small admixtures of nondirect processes. To determine the sensitivity of the 1^+ polarization measurement to the tensor force requires more precise optical parameters and, in addition, may require a more sophisticated calculation, including channel coupling, tensor exchange, and possibly intermediate structure.

APPENDIX

Scattering Amplitude Including a Tensor Force

In the presence of spin-orbit distorting potentials the projectile wave function will have the form

$$\chi_{iT'}^{(+)M'P'} = \sum_{L_1 N_1 J_1 M_1} 4\pi i^{L_1} Y_{L_1}^{N_1*}(\hat{k}) C(L_1 J'J_1; N_1 M'M_1)[Y_{L_1}(\hat{R}')\varphi_{J'T'}^{P'_1}]_{J_1}^{M_1} \mathfrak{R}_{J_1 L_1}(R'), \tag{A1}$$

where R' is the center of mass of the projectile. We have the task of calculating the DWBA amplitude

$$A_{M_i M_i', M_f M_f'} = \langle \chi_{fT'}^{(-)M_f P_f} \varphi_{J_f T_f}^{M_f P_f} |V| \varphi_{J_i T_i}^{M_i P_i} \chi_{iT'}^{(+)M_i' P_i'} \rangle \tag{A2}$$

in which V consists of both central and tensor terms, which we now consider in detail.

The tensor force between particle 1 in the target and particle 1' in the projectile is

$$V_T(\vec{r}) = S_{12} V_{12}(r)(V_{T0} + V_{T1}\vec{\tau}_1 \cdot \vec{\tau}_1'), \tag{A3}$$

where S_{12} is the tensor operator

$$S_{12} = \frac{3(\vec{\sigma}_1 \cdot \vec{r})(\vec{\sigma}_1' \cdot \vec{r})}{r^2} - \vec{\sigma}_1 \cdot \vec{\sigma}_1' = (24\pi/5)^{1/2} \sum_\beta S_2^\beta Y_2^{\beta*}(\hat{r}), \tag{A4}$$

with

$$S_2^\beta \equiv [\sigma_1 \sigma_1']_2^\beta, \tag{A5}$$

and $V_{12}(r)$ is a radial form factor, which for the one-pion force is a spherical Hänkel function

$$V_{12} = V_T h_2^{(1)}(i\alpha r). \tag{A6}$$

Since the quantity $Y_2^{\beta*}(\hat{r})V_{12}(r)$ is a second-rank tensor in the r space its expansion in R' and r_1 will have the general form

$$(24\pi/5)^{1/2} V_{12}(r)Y_2^\beta(\hat{r}) = \sum_{LN\lambda\mu} v_{L\lambda}(R', r_1)C(L\lambda 2; N\mu\beta)Y_{\lambda\mu}(\hat{r}_1)Y_{LN}(\hat{R}'). \tag{A7}$$

For the one-pion interaction the radial function is[12, 32, 33]

$$v_{L\lambda}(R', r_1) = (-1)^{\lambda+1} i^{\lambda-L} \times \tfrac{1}{5}\sqrt{6}(4\pi)^{3/2} \langle \lambda \| Y_2 \| L\rangle \begin{cases} j_\lambda(i\alpha r_1)h_L^{(1)}(i\alpha R') & R' > r_1 > 0 \\ j_L(i\alpha R')h_\lambda(i\alpha r_1) & 0 < R' < r_1 . \end{cases} \tag{A8}$$

The central exchange interaction we write as

$$V_C(r) = f(r)(V_{00} + V_{10}\vec{\sigma}_1' \cdot \vec{\sigma}_1 + V_{01}\vec{\tau}_1' \cdot \vec{\tau}_1 + V_{11}\vec{\sigma}_1' \cdot \vec{\sigma}_1 \vec{\tau}_1' \cdot \vec{\tau}_1). \tag{A9}$$

We first expand the spatial function

$$f(r) = \sum_{LM} v_L(R', r_1)Y_L^M(R')Y_L^{-M}(r_1)(-1)^M, \tag{A10}$$

where, for a Yukawa interaction $e^{-\alpha r}/\alpha r$

$$v_L = -4\pi j_L(i\alpha r_<)h_L^{(1)}(i\alpha r_>). \tag{A11}$$

In general, any over-all-scalar, charge-independent interaction can be written in the form[34]

$$V(1', 1) = \sum_{IN\tau\rho} T_{I\tau}^{-N-\rho}(1')T_{I\tau}^{N\rho}(1)(-1)^{N+\rho}f_{I\tau}, \tag{A12}$$

where $T_{I\tau}^{N\rho}$ is a rank-I tensor in ordinary space and a rank-τ tensor in charge space, and $f_{I\tau}$ is a scalar function of the coordinates. For the central and tensor forces it will be adequate to take

$$T^{N\rho}_{I\tau}(1') = \sum_{LI'}[Y_L(R')\mathbf{s}_{I'}(1')]^{N'}_{I'}\mathcal{T}^\rho_\tau(1'),$$

(A13)

where

$$\mathbf{s}^\mu_{I'} = \begin{cases} \sigma^\mu & I' = 1 \\ \delta_{I'0}\delta_{\mu 0} & I' = 0, \end{cases}$$

(A14a)

$$\mathcal{T}^\rho_\tau = \begin{cases} 2t^\rho & \tau = 1 \\ \delta_{\tau 0}\delta_{\rho 0} & \tau = 0, \end{cases}$$

(A14b)

where $\tfrac{1}{2}\sigma^\mu$ and t^ρ are the spherical components of the nuclear spin and isospin operators, respectively.

We can obtain the form (A12) for the central and tensor forces by using the expansions in spherical harmonics [Eqs. (A7) and (A10)], recoupling the spin operator and spherical harmonic of each coordinate together first, and then coupling the resulting operators:

$$V_C = \sum_{INI'I\tau\rho}(-1)^{N+\rho}(-1)^{I-I'-L}[Y_L(R')\mathbf{s}_{I'}(1')]^{-N}_I\mathcal{T}^{-\rho}_\tau(1')V_{I'\tau}v_L(R',r_1)[Y_L(\hat{r}_1)\mathbf{s}_{I'}(1)]^N_I\mathcal{T}^{-\rho}_\tau(1),$$

(A15a)

$$V_T = \sum_{IN\tau\rho L}(-1)^{N+\rho}[Y_L(\hat{R}')\sigma(1')]^{-N}_I\mathcal{T}^{-\rho}_\tau(1')\sum_\lambda 5V_{T\tau}(-1)^{L+1}W(L\lambda 11;2I)v_{L\lambda}(R',r_1)[\hat{Y}_\lambda(r_1)\sigma(1)]^N_I\mathcal{T}^\rho_\tau(1).$$

(A15b)

The two may be combined in a single form like Eq. (A12) but with a little more detail:

$$V = \sum_{II'L\lambda}\left[\sum_{N\rho}(-1)^{N+\rho}T^{-N}_{I(LI')}(1')\mathcal{T}^{-\rho}_\tau(1')T^N_{I(\lambda I)}\mathcal{T}^\rho_\tau(1)\right](-1)^{I-I'-L}F_{II'L\lambda\tau}(R',r_1),$$

(A16)

where

$$T_{I(LI')}(1') = [Y_L(R')\mathbf{s}_{I'}(1')]^N_I$$

(A17)

and

$$F_{II'L\lambda\tau} = \delta_{L\lambda}V_{I'\tau}v_\lambda(R',r_1) + 5(-1)^IV_{T\tau}\delta_{I'1}W(L\lambda 11;2I)v_{L\lambda}(R',r_1).$$

(A18)

We now write the potential in a second-quantized form:

$$V = \sum\langle j_2 m_2\alpha_2,\tfrac{1}{2}\nu_2\beta_2|V|j_1 m_1\alpha_1;\tfrac{1}{2}\nu_1\beta_1\rangle a^\dagger_{j_2 m_2\alpha_2}a_{j_1 m_1\alpha_1}c^\dagger_{\nu_2\beta_2}c_{\nu_1\beta_1}.$$

(A19)

With the help of Eq. (A16) we may calculate the two-particle matrix element as

$$\langle j_2 m_2\alpha_2,\tfrac{1}{2}\nu_2\beta_2|V|j_1 m_1\alpha_1;\tfrac{1}{2}\nu_1\beta_1\rangle = \sum_{INLM\lambda I'N'\tau\rho}(-1)^{N+\rho+I-I'-L}C(LI'I;MN'-N)Y^M_L(R)$$

$$\times \sum_{\alpha_1\alpha_2\beta_1\beta_2}\sum C(\tfrac{1}{2}\tfrac{1}{2}\tau;\beta_1-\beta_2+\rho)(-1)^{(1/2)-\beta_1}C(\tfrac{1}{2}\tfrac{1}{2}\tau;\alpha_1-\alpha_2-\rho)(-1)^{(1/2)-\alpha_1}$$

$$\times \sum_{j_1 j_2 m_1 m_2\nu_1\nu_2}C(j_1 j_2 I;m_1-m_2-N)^{j_1-m_1}C(\tfrac{1}{2}\tfrac{1}{2}I';\nu_1-\nu_2-N)$$

$$\times (-1)^{(1/2)-\nu_1}\frac{\langle\tfrac{1}{2}\|\mathbf{s}_{I'}\|\tfrac{1}{2}\rangle}{\hat{I}'}\frac{\langle\tfrac{1}{2}\|\mathcal{T}_\tau\|\tfrac{1}{2}\rangle^2}{\hat{\tau}^2}\frac{\langle j_2\|T_{I(\lambda I')}\|j_1\rangle}{\hat{I}}G^{j_1 j_2}_{II'L\lambda\tau}(R'),$$

(A20)

where

$$G^{j_1 j_2}_{II'L\lambda\tau} = \int \mathcal{R}_{j_2 l_2}(r_1)F_{II'L\lambda\tau}(R',r_1)\mathcal{R}_{j_1 l_1}(r_1)r_1^2 dr_1.$$

(A21)

The spin or isospin reduced matrix element is

$$\frac{\langle\tfrac{1}{2}\|\mathbf{s}_{I'}\|\tfrac{1}{2}\rangle}{\hat{I}'} = \sqrt{2}$$

(A22)

and the reduced matrix element of $T_{I(\lambda I')}$ is[35]

$$\langle j_2\|T_{I(\lambda I')}\|j_1\rangle = \sqrt{2}\,\hat{j}_1\hat{j}_2\hat{I}\hat{I}'\begin{pmatrix} j_1 & \tfrac{1}{2} & l_1 \\ j_2 & \tfrac{1}{2} & l_2 \\ I & I' & \lambda \end{pmatrix}\langle l_2\|Y_\lambda\|l_1\rangle.$$

(A23)

Taking advantage of the Clebsch-Gordan coefficients in Eq. (A20), we may rewrite the interaction Eq.(A19)

$$V = \sum_{L\lambda II'\tau}(-1)^{I-I'-L}2^{3/2}\hat{I}^{-1}\sum_{j_1 j_2}\langle j_2\|T_{I(\lambda I')}\|j_1\rangle G^{j_1 j_2}_{IL\lambda\tau}(R')\sum_{\rho N}A_{IN\tau\rho}(j_1 j_2)[Y_L(R')C_{I',\tau-\rho}]^{-N}_I(-1)^{\rho+N},$$

(A24)

where the tensors $A_{IN\tau\rho}(j_1 j_2)$ and $C_{I'N'\tau\rho}$ are the single-particle transition operators defined in Ref. 17. The over-all scalar form of the assumed interaction is evident from the form Eq. (A24).

With the help of Eq. (A24) it is easy to make a formal calculation of the scattering amplitude. The operator $A_{IN\tau\rho}$ operates only on the target nuclear states, and the operator $[Y_L(\hat{R}')C_{I',\tau-\rho}]_I^N$ operates only on the coupled wave function of the internal projectile coordinates and the orbital coordinates of Eq. (A1).

The target-nuclear part of Eq. (A2) is

$$\langle \varphi_{J_f}^{M_f} | A_{IN\tau\rho}(j_1 j_2) | \varphi_{J_i}^{M_i} \rangle = C(J_i J_f I; M_i - M_f - N)(-1)^{J_i - M_i} C(T_i T_f \tau; P_i - P_f - \rho)(-1)^{T_i - P_i} S(J_i J_f I; T_i T_f \tau; j_1 j_2).$$
(A25)

The spectroscopic amplitude is as defined in Ref. 17. The projectile part of the matrix element has a matrix element[35]

$$\langle [Y_{L_2}(R')\varphi_{J'T'}^{P_f'}]_{J_2}^{M_2} | [Y_L(R')C_{I',\tau-\rho}]_I^{-N} | [Y_{L_1}(R')\varphi_{J'T'}^{P_i'}]_{J_1}^{M_1} \rangle$$

$$= C(J_1 J_2 I; M_1 - M_2 N)(-1)^{J_1 - M_1} C(T'T'\tau; P_i' - P_f' \rho)(-1)^{T' - P_i'} S'(J'I'; T'\tau)\hat{J}_1\hat{J}_2\hat{I}' \begin{pmatrix} J_1 & J' & L_1 \\ J_2 & J' & L_2 \\ I & I' & L \end{pmatrix} \langle L_2 \| Y_L \| L_1 \rangle,$$
(A26)

where $S'(J'I'; T'\tau)$ is the projectile spectroscopic amplitude.[17] Putting together the results of Eqs. (A24), (A25), and (A26) we have an expression for the scattering amplitude, Eq. (A2).

$$A_{M_i M_i', M_f M_f'} = \sum_{\substack{L_1 N_1 J_1 M_1 \\ L_2 N_2 J_2 M_2 \\ INI'L}} C(J_i J_f I; M_i - M_f - N)(-1)^{J_i - M_i}(-1)^{N + I - L' - L}(4\pi)^2 i^{L_1 - L_2} Y_{L_1}^{N*}(\hat{k}_i)$$

$$\times Y_{L_2}^{N_2}(\hat{k}_f) C(L_1 J' J_1; N_1 M_i' M_1) C(L_2 J' J_2; N_2 M_f' M_2) C(J_1 J_2 I; M_1 - M_2 N)(-1)^{J_1 - M_1}\frac{\hat{J}_1 \hat{J}_2 \hat{I}'}{\hat{I}}$$

$$\times \begin{pmatrix} J_1 & J' & L_1 \\ J_2 & J' & L_2 \\ I & I' & L \end{pmatrix} \langle L_2 \| Y_2 \| L_1 \rangle \int \Re_{J_2 L_2}(R') G_{II'L}(R') \Re_{J_1 L_1}(R') R'^2 dR',$$
(A27)

where

$$G_{II'L}(R') = \sum_{\tau\rho} C(T'T'\tau; P_i' - P_f'\rho)(-1)^{T' - P_f'} S(J'I'; T'\tau) \sum_{j_1 j_2 \lambda} (2^{3/2})\langle j_2 \| T_{I(\lambda I')} \| j_1 \rangle$$

$$\times C(T_i T_f \tau; P_i - P_f - \rho)(-1)^{T_i - P_i} S(J_i J_f I; T_i T_f \tau; j_1 j_2) G_{II'L\lambda\tau}^{j_1 j_2}(R').$$
(A28)

We finally simplify slightly by taking $\hat{k}_i = \hat{0}$, so $N_1 = 0$ and replacing N_2 by M. We have then

$$A_{M_i M_i', M_f M_f'} = \sum_{IN} C(J_i J_f I; M_i - M_f - N)(-1)^{J_i - M_i} \alpha(M_i' M_f' IN),$$
(A29)

where

$$\alpha(M_i' M_f' IN) = \sum_{L_1 L_2 M J_1 J_2 I'L} (4\pi)^2 i^{L_1 - L_2}(-1)^{N + I - I' - L} Y_{L_1}^0(\hat{0}) Y_{L_2}^M(\hat{k}_f) C(L_1 J' J_1; 0 M_i' M_i')$$

$$\times C(L_2 J' J_2; M, M_f', M + M_f')(-1)^{J_1 - M_i'} C(J_1 J_2 I; M_i', -M - M_f', N)\frac{\hat{J}_1 \hat{J}_2 \hat{I}'}{\hat{I}}$$

$$\times \begin{pmatrix} J_1 & J' & L_1 \\ J_2 & J' & L_2 \\ I & I' & L \end{pmatrix} \langle L_2 \| Y_L \| L_1 \rangle \int \Re_{J_2 L_2}(R') G_{II'L}(R') \Re_{J_1 L_1}(R') R'^2 dR'.$$
(A30)

The differential cross section is coherent in I' and L but incoherent in IN:

$$\frac{d\sigma}{d\Omega} = \left(\frac{2m}{2\pi\hbar^2}\right)^2 \frac{k_f}{k_i} \frac{1}{(2J_i + 1)(2J' + 1)} \sum_{INM_i'M_f'} |\alpha(M'M'IN)|^2.$$
(A31)

The triangle inequalities satisfied by the various transfer quantum numbers are $\Delta(Ij_1 j_2)$, $\Delta(IJ_i J_f)$, $\Delta(IJ_1 J_2)$, $\Delta(\lambda l_1 l_2)$, $\Delta(\lambda II')$, $\Delta(LL_1 L_2)$, $\Delta(LII')$, $\Delta(I'\frac{1}{2}\frac{1}{2})$, $\Delta(\tau\frac{1}{2}\frac{1}{2})$, $\Delta(\tau T_i T_f)$. An additional restriction comes from the parity rule

$$(-1)^\lambda = (-1)^L = (-1)^{\Delta\pi}.$$
(A32)

In a problem where the spin-dependent distorting potentials can be neglected the dependence of the radial

wave functions on J_1 and J_2 will disappear. In that case we can carry out the $J_1 J_2$ sum in Eq. (A27); however, it is easier to go back to the interaction Eq. (A24) and evaluate the amplitude for a spin-independent distorted wave. The resulting cross section is incoherent in I, I', and L:

$$\frac{d\sigma}{d\Omega} = \left(\frac{2m}{4\pi\hbar^2}\right)^2 \frac{k_f}{k_i} \frac{1}{(2J_i+1)(2J'+1)} \sum_{II'LM} |\langle \chi_f^{(-)} |G_{II'L}(R')Y_L^M(R')| \chi_i^{(+)} \rangle|^2 , \tag{A33}$$

where the χ are purely spatial distorted wave functions. This form is probably adequate for $(^3\mathrm{He}, t)$, since spin-orbit forces contribute relatively little to the optical potential.

---

*Work performed under the auspices of the U. S Atomic Energy Agency.

†Present address: Physics Department, Case Western Reserve University, Cleveland, Ohio 44106.

[1]C. Wong, J. D. Anderson, J. McClure, B. Pohl, V. A. Madsen, and F. Schmittroth, Phys. Rev. 160, 769 (1967).

[2]J. D. Anderson, S. D. Bloom, C. Wong, W. F. Hornyak, and V. A. Madsen, Phys. Rev. 177, 1416 (1969).

[3]A. M. Lane, Phys. Rev. Letters 8, 171 (1962); Nucl. Phys. 35, 676 (1962).

[4]S. D. Bloom, J. D. Anderson, W. F. Hornyak, and C. Wong, Phys. Rev. Letters 15, 264 (1965).

[5]V. A. Madsen, in Proceedings of the Second Conference on Nuclear Isospin, Asilomar-Pacific Grove, California, 13-15 March 1969, edited by J. D. Anderson, S. D. Bloom, J. Cerny, and W. W. True (Academic Press Inc., New York, 1969).

[6]J. Atkinson and V. A. Madsen, Phys. Rev. C 1, 1377 (1970).

[7]W. M. Visscher and R. A. Ferrell, Phys. Rev. 107, 781 (1957).

[8]D. R. Inglis, Rev. Mod. Phys. 25, 390 (1953).

[9]H. J. Rose, O. Häusser, and E. K. Warburton, Rev. Mod. Phys. 40, (1968).

[10]G. C. Ball and J. Cerny, Phys. Rev. 177, 1466 (1969).

[11]J. Atkinson and V. A. Madsen, Phys. Rev. Letters 21, 295 (1968).

[12]F. A. Schmittroth, Ph.D. thesis, Oregon State University, 1968 (unpublished).

[13]B. D. Walker, C. Wong, J. D. Anderson, J. W. McClure, and R. W. Bauer, Phys. Rev. 137, B347 (1965).

[14]In Fig. 1 of Ref. 13, a "left" scattering occurs when P_1 is rotated $+\frac{\pi}{2}$ such that P_1 and P_2 are parallel. Similarly a "right" scattering occurs when P_1 is rotated $-\frac{\pi}{2}$ such that P_1 and P_2 are antiparallel.

[15]For a discussion of the polarization sign convention and a determination of the direction of precession see Ref. 13.

[16]A similar derivation of the cross section with a two-body tensor interaction by W. G. Love and L. J. Parish has appeared in preprint form. These authors also include the knockout contribution.

[17]V. A. Madsen, Nucl. Phys. 80, 177 (1966).

[18]G. R. Satchler, Nucl. Phys. 55, 1 (1964).

[19]B. A. Watson, P. P. Singh, and R. E. Segel, Phys. Rev. 182, 977 (1969).

[20]E. H. Schwarcz, Phys. Rev. 149, 752 (1966).

[21]R. W. Bauer, J. D. Anderson, H. F. Lutz, C. Wong, J. W. McClure, and B. A. Pohl, Nucl. Phys. A93, 673 (1967).

[22]M. A. Nagarajan and J. Hanna, private communication.

[23]G. M. Crawley, S. M. Austin, W. Benenson, V. A. Madsen, F. A. Schmittroth, and M. J. Stomp, to be published.

[24]From the $^{14}\mathrm{C}(p, n)$ ground-state cross section calculated with a regularized one-pion form factor with $\beta = 2$, an estimate of the cross section with $\beta = 4$, on the basis of r^2 weighted volume integrals, gives a result higher by about 17%.

[25]S. Cohen and D. Kurath, Nucl. Phys. 73, 1 (1965).

[26]A. Arima, S. Cohen, R. D. Lawson, and M. H. MacFarlane, Nucl. Phys. A108, 94 (1968).

[27]W. G. Love, L. J. Parish, and A. Richter, Phys. Letters 31B, 167 (1970).

[28]F. Petrovich, H. McManus, V. A. Madsen, and J. Atkinson, Phys. Rev. Letters 22, 895 (1969).

[29]G. R. Satchler, Nucl. Phys. A100, 497 (1967).

[30]A. Agassi and R. Schaeffer, Phys. Letters 26B, 703 (1968).

[31]J. D. Anderson, C. Wong, and V. A. Madsen, Phys. Rev. Letters 24, 1074 (1970).

[32]A. K. Kerman, private communication.

[33]P. J. A. Buttle and L. J. B. Goldfarb, Nucl. Phys. 78, 409 (1966).

[34]G. R. Satchler, Nucl. Phys. 77, 481 (1966).

[35]A. R. Edmonds, Angular Momentum in Quantum Mechanics (Princeton University Press, Princeton, New Jersey, 1957).